Dosimetric Investigation of Six Ru-106 Eye Plaques by EBT3 Radiochromic Films and Monte Carlo Simulation

Mojtaba Arjmand (MSc)[1]*, Fariba Ghassemi (MD)[2], Payman Rafiepour (MSc)[3], Reyhaneh Zeinali (MSc)[4], Hamid Riazi-Esfahani (MD)[1,5], Akbar Beiki-Ardakani (PhD)[6]

[1]Ocular Oncology service, Farabi Eye Hospital, Tehran University of Medical Sciences, Tehran, Iran
[2]Retina & Vitreous Service-Ocular Oncology Service, Farabi Eye Hospital, Tehran University of Medical Sciences, Tehran, Iran
[3]Department of Nuclear Engineering, Shiraz University of Medical Sciences, Shiraz, Iran
[4]Department of Medical Physics, Tabriz University of Medical Science, Tabriz, Iran
[5]Retina Service, Farabi Eye Hospital, Tehran University of Medical Sciences, Tehran, Iran
[6]Radiation Medicine Program, Princess Margaret Cancer Centre, University Health Network, Toronto, Ontario, Canada

ABSTRACT

Background: Ophthalmic brachytherapy using radioactive plaques is an effective technique for the treatment of uveal melanoma. Ru-106 eye plaques are considered as interesting issue due to their steep gradient dose. The pre-planning evaluation of dosimetric parameters is essential for the treatment planning system.

Objective: The current study aims at providing dose distributions of six Ru-106 eye plaques (CCA, CCB, CGD, CIB, COB and COD) using radiochromic EBT3 film, Geant4 Monte Carlo toolkit and the treatment planning software (Plaque Simulator).

Material and Methods: In this experimental study, an in-house phantom was employed for depth dose measurements with EBT3 films. Also, Geant4.10.5 scoring mesh was implemented to obtain the 2D dose distribution of the plaques. The results were compared with Plaque Simulator software and the manufacturer's (BEBIG) data. The gamma index criterion (3%/3 mm) was used to evaluate dose distributions obtained by the film measurements and Geant4 simulation.

Results: A good agreement was achieved between simulation and experimental results. Gamma index passing rate was 94.2%, 89.3%, 88.2%, 82.2%, 92.2% and 90.1% for CCA, CCB, CGD, CIB, COB and COD plaques, respectively. Absolute dose rate (mGy/min) obtained by EBT3 film at the depth of 2 mm was 79.4 mGy/min, 81.0 mGy/min, 78.6 mGy/min, 62.2 mGy/min, 75.2 mGy/min and 81.2 mGy/min for CCA, CCB, CGD, CIB, COB and COD plaques, respectively.

Conclusion: The measured dose distributions and lateral dose profiles may be utilized in the treatment planning system to cover clinical volumes such as the clinical target volume and the gross tumor volume.

Citation: Arjmand M, Ghassemi F, Rafiepour P, Zeinali R, Riazi-Esfahani H, Beiki-Ardakani A. Dosimetric Investigation of Six Ru-106 Eye Plaques by EBT3 Radiochromic Films and Monte Carlo Simulation. *J Biomed Phys Eng*. 2023;13(4):309-316. doi: 10.31661/jbpe.v0i0.2010-1206.

Keywords

Uveal Melanoma; Ru-106 Plaque; Dosimetry; Brachytherapy; EBT3 Film; Monte Carlo Method

Introduction

Uveal melanoma is a deadly malignancy, rising from the basal cells within uveal tract of the eye. The mean annual incidence of this malignancy was reported about 5.1 cases per 10^6 in the United States [1], 2-8 cases per 10^6 in Europe [2] and 0.2-0.3 cases per 10^6 in Africa and Asia [3]. Brachytherapy using eye plaques is an effective treatment approach for ocular tumors [4]. Different radioisotopes such as I-125, Cs-131, Pd-103, Sr-90 and Ru-106 and different plaque models have been employed for this technique [5]. Among them, both

*Corresponding author:
Mojtaba Arjmand
Ocular Oncology Service, Farabi Eye Hospital, Tehran University of Medical Sciences, Tehran, Iran
E-mail: arjmand.mojtaba@gmail.com

Received: 11 October 2020
Accepted: 10 February 2021

Ru-106 coated and I-125 seed-loaded plaques were widely used for clinical needs [6-9]. The choice of plaque type depends on the tumor size and the location as well as dosimetric studies prior to the treatment planning. Dosimetric investigation of the plaques before the treatment planning is highly important especially for beta emitting ones. In the case of small ocular tumors and the tumors adjacent to the sensitive structures (e.g. optic nerve, lens and cornea), beta emitting plaques have been shown to be superior to the photon emitting ones, due to their steep dose gradient sparing nearby tissues [10]. Radiochromic films are known as interesting dosimeters for such high gradient radiation fields because of their high spatial resolution. Several dosimetric investigations for Ru-106 plaques were done in the past few years, using radiochromic films [11-13] and other dosimeters [14-18] as well as Monte Carlo simulation [19-20]. The limitation of these studies (except ref. 20) is that the dosimetric investigation was conducted only for a few (often CCA and CCB) Ru-106 plaque types. In this study, the dose distributions of CCA, CCB, CGD, CIB, COB and COD plaques were investigated using radiochromic EBT3 films, Geant4 Monte Carlo toolkit and Plaque Simulator as the treatment planning software (TPS). Depth dose measurements were obtained for all plaques and compared with the manufacturer (BEBIG) results. The gamma index (GI) with 3% local dose difference and 3 mm distance-to agreement criterion [21] was employed to evaluate the dose distributions achieved by film measurements and Geant4 simulation.

Material and Methods

Ru-106 eye plaques

Six Ru-106 plaques produced by the Eckert & Ziegler BEBIG company in Germany (www.bebig.com) were employed in this experimental study (Figure 1). Each plaque model was designed for specific tumors, including the tumors of uvea (CCA, CCB and CGD plaques), the tumors close to the optic nerve (COB and COD plaques) and the tumors near the iris (CIB plaque). The plaques consist of 0.1 mm silver window, 0.2 mm Ru-106 coated foil and 0.7 mm silver backing [22]. Ru-106 is a pure beta emitter, decaying to Rh-106, with a half-life ($T_{1/2}$) of about one year. Rh-106 decays to Pd-106, with a half-life of 29.8 s. The maximum beta energy of Ru-106 and Rh-106 is 0.39 MeV and 3.53 MeV, respectively. Rh-106 also has some gamma rays in its decay scheme [23]. Table 1 represents the dimensions and the initial activities of the

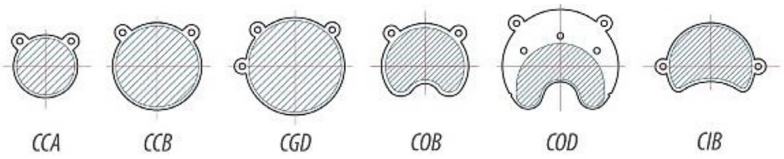

Figure 1: Six Ruthenium-106 plaques of BEBIG company, which are used in this study. Used with permission from Eckert & Ziegler BEBIG [22].

Table 1: Geometrical characteristics of six Ruthenium-106 plaques.

	CCA	CCB	CGD	COB	COD	CIB
Diameter (mm)	15.30	20.20	22.30	19.80	25.40	20.20
Active diameter (mm)	14.30	19.80	21.30	17.80	15.40	19.80
Spherical radius (mm)	12.00	12.00	13.00	12.00	14.00	12.00
Initial activities (MBq)	11.85	21.09	36.74	16.78	20.68	19.28

plaques.

Radiochromic EBT3 film measurements

EBT3 film is the third member of EBT radiochromic films family, developed to be more accurate and reliable, and consists of an active layer with 28 μm thickness, compressed between two layers of Matte Polyester with a thickness of 125 μm [24]. They have the advantages of near soft tissue equivalence, high spatial resolution and small energy dependence, causing them to be desirable for dosimetric studies in radiation fields with steep dose gradients. The Newton rings effect due to the direct contact of the film with the glass surface of the scanner was eliminated in EBT3 film by embedding silica particles within its polyester layers. The symmetrical structure and the anti-Newton rings feature are known as the advantages of EBT3 films compared to the previous models [25]. For film calibration, eight pieces of 2.5×2.5 cm^2 were cut from one sheet (lot number 03111902) and being exposed by a 6 MV linear accelerator at a depth of 10 cm in a water equivalent phantom (with the source to surface distance of 100 cm and radiation field of 10×10 cm^2). A range of dose from 0.5 to 10 Gy was delivered to the films. One piece of film was kept unexposed for background measurement. The films were marked to keep the same orientation for all pieces and cut carefully with small scissors, handled with gloves and stored in a safe place for 24 h before processing to ensure the response stability [25].

An Epson Expression 10000XL flatbed scanner was used in this study. Using flatbed scanners as a readout system for radiochromic films, causes common artifacts: The dependence of scanner response on the film orientation on the scanner bed (the orientation effect) and the parabolic change of scanner response by the lateral offset from the scanner midline (the lateral effect) [26]. The orientation of the films was marked carefully. All EBT3 film pieces were located at the center of the scanning bed with the same orientation to reduce these artifacts. Prior to scanning, several empty scans were done for warming up the scanner. Although, the Callier effect due to the flatness of the film on the scanning bed may affect the film response [27], The Epson Expression 10000XL scanners have a pressed glass sheet on the inner surface of their lid to mitigate this effect. EBT3 films were digitized using RGB 48-bit mode (16-bit color depth per Red, Green and Blue color channels) with 72 dots per inch (dpi) scanning resolution in the transmission mode. Images were saved in TIFF (uncompressed tagged image file) format. The mean pixel value (PV) of a region of interest (ROI) of 1.5×1.5 cm^2 was read with ImageJ software (version 1.5). All PVs were obtained in red channel due to the highest sensitivity of active layer to the red wave length [25]. The net optical density (nOD) was calculated by equation 1:

$$nOD=\log_{10}(PV_{bef}/PV_{aft}) \quad (1)$$

In which, PV_{bef} and PV_{aft} are the average PVs over the ROIs of scanned images before and after the exposure, respectively [25].

An in-house water equivalent (PMMA) phantom (Z_{eff}=6.48) with dimensions of 4×4×4 cm^3 and 1.18 g/cm^3 density was utilized for depth dose measurements. It has a spherical cab with 12 mm radius to fit the shape of plaques. As shown in Figure 2, the phantom consists of three parts to allow the measurement of depth dose profile along the central axis of the films. A PMMA holder was added to the phantom configuration to account the backscattering radiation.

Radiochromic film calibration equation was obtained by fitting a third order polynomial function on the dose vs nOD data (Equation 2). Measuring nOD of each point of the scanned images and substituting it in the calibration curve equation results the absorbed dose in that point. Then dose rate is calculated by Equation 3:

$$D=554.596(nOD)^3-36.0459(nOD)^2+15.121(nOD)+0.0643,\ (R^2=0.999) \quad (2)$$

$$\dot{D}\left(\frac{mGy}{min}\right)=(D/T_{irr})\times e^{-\lambda T_{irr}}\times(1000/60) \quad (3)$$

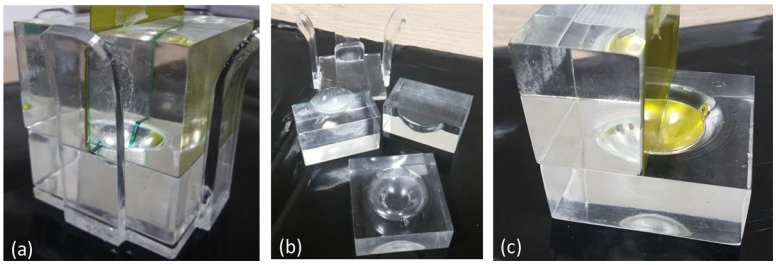

Figure 2: a) The whole phantom configuration, b) The phantom segments and c) Depth dose measurement set-up with EBT3 film and a dummy plaque.

In which, D (Gy) is the dose obtained by calibration curve equation, T_{irr} (hr) is the exposure time, and λ (hr^{-1}) is the decay constant equal to $0.693/T_{1/2}$. The exponential term is the decay factor of the plaques, implemented due to the decay of Ru-106 during exposure time. The involved uncertainties include the uncertainty originated from measuring film response to radiation, the fitting procedure of the calibration curve, the phantom and the plaque wrong assembly, Linac error in delivery and lack of uniformity of the exposure to the reference films. We tried to keep the total uncertainty below 10%.

Monte Carlo simulation

Geant4.10.5 Monte Carlo toolkit with Livermore low energy physics model (G4EmLivermorePhysics) was used in this study. The Livermore physics model includes photoelectric effect, pair production, Compton and Rayleigh scattering, bremsstrahlung, ionization and fluorescence emission [28]. Auger electron from excited atoms was implemented in the physics list, via macro file [29]. Range cut value was set to 0.5 mm for photons, electrons and positrons, i.e. the tracking of secondary particles with the range of less than 0.5 mm ceased and their energy was deposited locally.

The radioactive plaques were simulated in a large cubic water phantom with 10×10×10 cm^3 dimension. The box scoring mesh of Geant4 was implemented to obtain 2D dose profile of the plaques. As the scanning resolution of the scanner (72 dpi) corresponds to 2.85 pixels per mm, the mesh bins have been defined with a dimension of 0.35×0.35×0.35 mm^3. Each division was performed for different radial distances. Furthermore, twenty spherical detectors with 0.25 mm diameter were defined at 0.5 mm intervals for the depth dose measurements. The completed Ru-106 decay scheme was simulated by employing the ability of Geant4 in the simulation of radioisotope decay. As the half-life of Ru-106 is much greater than the Ru-106 half-life, the secular equilibrium of the daughter occurs, i.e. the instantaneous amount of Rh-106 transforming is equal to that of Ru-106 [30]. Therefore, complete Ru-106 and Rh-106 decay schemes were simulated. The primary particles generated by Ru-106 were set to 6×10^8 and all statistical errors in Geant4 simulations were below 3% up to the depth of 8 mm. Dose reference point was considered at 2 mm depth on the central axis of the plaques and the prescription dose was reported in the range of 70-100 Gy for tumors with 5 mm apex [5].

GI analysis 3%/3 mm criterion was employed to evaluate dose distributions of Ru-106 plaques. This pixel-to-pixel comparison was performed between EBT3 films and Geant4 results as the reference and the evaluated dose distributions, respectively. It consists of two concepts, performing simultaneously as follows: firstly, a point-by-point calculation of the dose difference between two dose distributions, with an acceptable dose difference of 3% of the maximum dose. Secondly, a measurement of spatial distance between two closest points of the same dose in the reference and the evaluated dose distributions, with

an acceptable spatial tolerance of 3 mm [21].

Results

Two-dimensional dose profiles of Ru-106 plaque types are represented in Figure 3. The relative dose is normalized to its maximum value for each plaque.

A comparison of relative depth dose, normalized at the reference point and obtained by EBT3 film, Geant4, Plaque Simulator (TPS) and BEBIG data is presented in Figure 4. According to the BEBIG calibration certificate, 20% uncertainty was added to its data, as shown with error bars in Figure 4.

Figure 5 shows the GI maps calculated with 3%/3 mm criterion using MATLAB 9.0 code. Lateral dose profiles of six Ru-106 plaques obtained by EBT3 film are shown in Figure 6. The absolute dose rates (mGy/min) at the reference point obtained by film measurements, Geant4 simulation and from the manufacturer are tabulated in Table 2.

Discussion

Figure 3 demonstrates that the dose distribution of the plaques is highly affected by the shape and the size of the plaques, depending on the tumor location and its size. The 10% isodoses extends to 4 mm depth except for CGD plaques, which has the largest active diameter. It shows that CGD plaques may be preferred for large tumors up to 5 mm depth. A good agreement is achieved between the relative dose rates shown in Figure 4. This agreement accentuates the validation of our experimental and simulation study. All the results are confined in 20% error bars proposed by the manufacturer, up to the depth of 10 mm. However, a little deviation was observed for the results of Geant4 simulation of COD plaque at 9 mm and 10 mm depths. Finally, a quantitative comparison was done between Geant4 simulation results and EBT3 film measurements. The GI evaluation, presented in Figure 5, shows the adaptable dose distributions, obtained experimentally and by simulation. In a quality assurance scenario, the gamma index passing rate (GIPR), which is the percentage of total points that achieved GI<1, is defined as a pass/fail test for a given GI criterion (e.g. 3%/3 mm) [31]. GIPR was 94.2%, 89.3%, 88.2%, 82.2%, 92.2% and 90.1% for CCA, CCB, CGD, CIB, COB and COD plaques, respectively. For GI with 5%/5 mm criterion, the GIPR was 97.9%, 98.8%, 95.9%, 91.7%, 96.6% and 96.8% for CCA, CCB, CGD, CIB, COB and

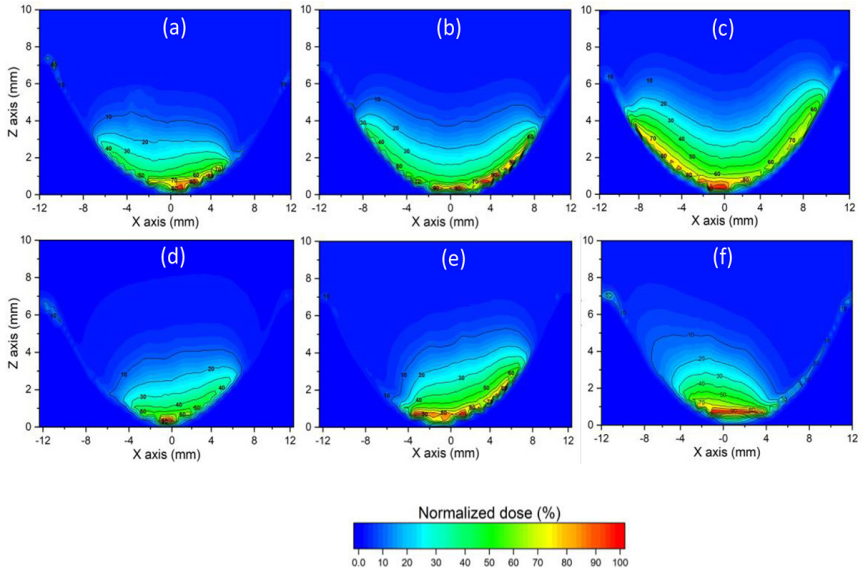

Figure 3: 2D Dose profiles of a) CCA, b) CCB, c) CGD, d) CIB, e) COB and f) COD Ruthenium-106 plaques.

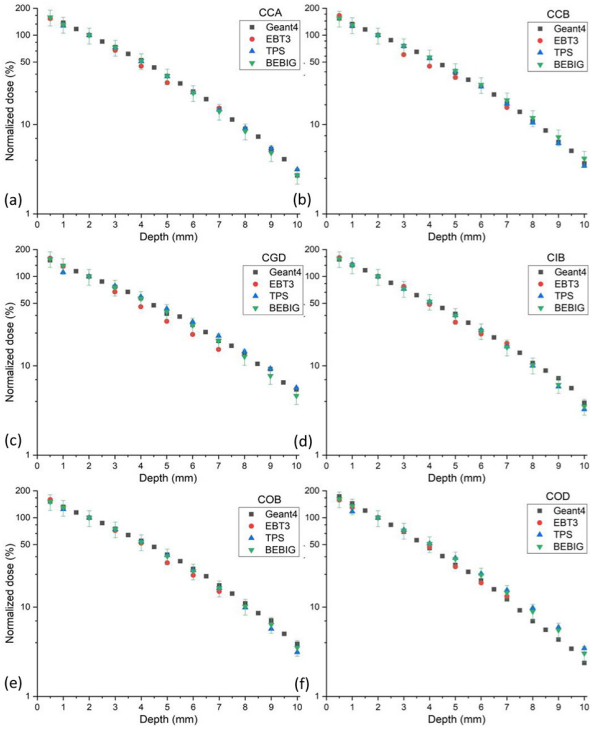

Figure 4: Relative dose rate comparisons with BEBIG results for a) CCA, b) CCB, c) CGD, d) CIB, e) COB and f) COD Ruthenium-106 plaques.

COD plaques, respectively. All relative errors between calculated dose rates tabulated in Table 2 are below 10%, except for COD plaque. It seems to be due to its specific geometry, making the simulation more complicated. Note that the BEBIG data were obtained using plastic scintillators. Moreover, this study shows that EBT3 radiochromic film may be an alternative detector with high spatial resolution for such high dose gradient fields.

Conclusion

In this work, a dosimetric study of six brachytherapy Ru-106 plaques was performed using radiochromic EBT3 film, Geant4 Monte Carlo simulation and Plaque Simulator software. The obtained dose distributions show that radiochromic EBT3 film with high spatial resolution is an appropriate dosimeter for beta emitting eye plaques. The results of Monte Carlo simulation, EBT3 films and TPS were in a good agreement with BEBIG data. The measured 2D dose distributions and lateral dose

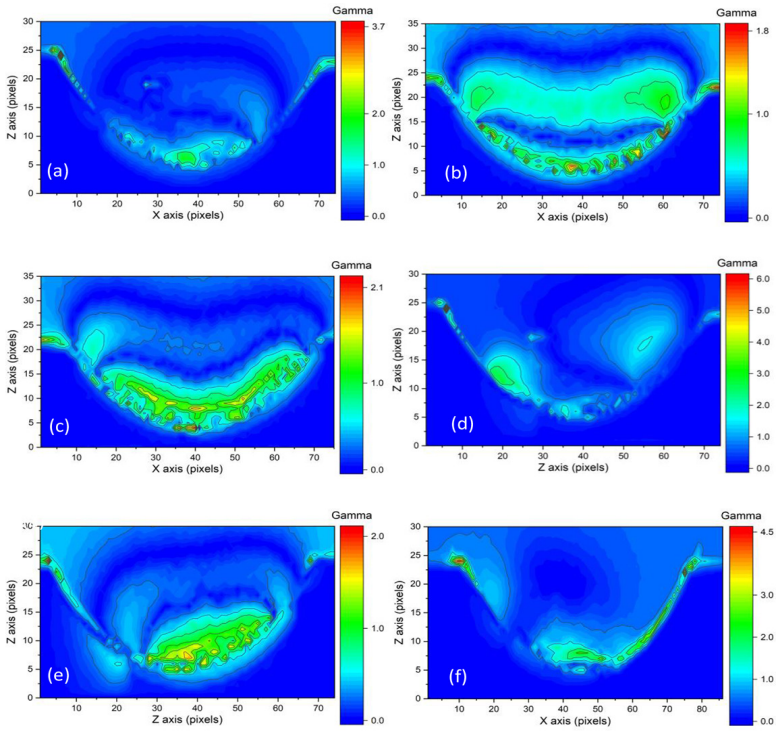

Figure 5: The evaluation of 2D dose profiles of a) CCA, b) CCB, c) CGD, d) CIB, e) COB and f) COD plaques obtained by EBT3 films and Geant4, using 3%/3 mm gamma index (GI) analysis.

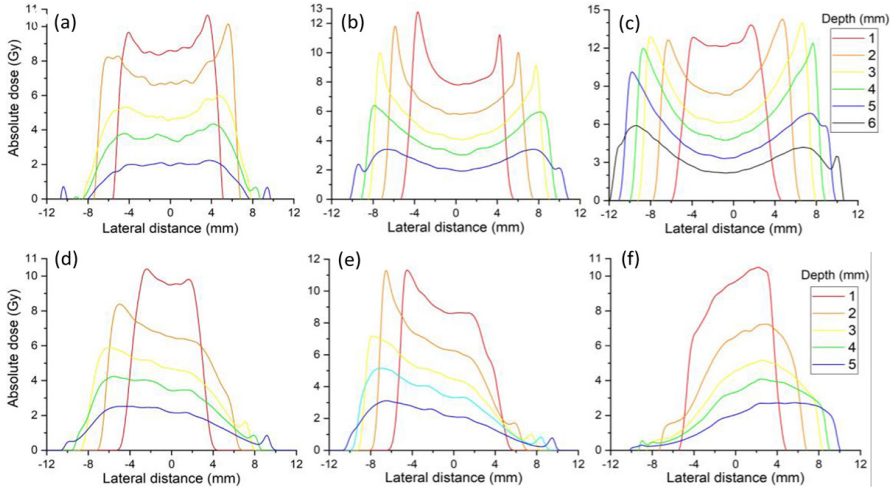

Figure 6: Lateral dose profiles of a) CCA, b) CCB, c) CGD, d) CIB, e) COB and f) COD plaques.

Table 2: Absolute dose rates (mGy/min) at the reference point obtained by EBT3 film, Geant4 and from the manufacturer for six Ru-106 plaques.

	CCA	CCB	CGD	CIB	COB	COD
EBT3 film	79.4	81.0	78.6	62.2	75.2	81.2
Geant4	83.7	81.5	79.1	60.7	70.4	95.2
BEBIG	84.4	85.7	81.5	65.8	76.9	89.5

profiles may be used in the treatment planning system for covering clinical volumes such as the clinical target volume and the gross tumor volume.

Authors' Contribution

M. Arjmand performed the experimental work, wrote the manuscript and interpreted the results. F. Ghassemi was a major contributor in writing and designing the manuscript and proposed the idea of the study. P. Rafiepour performed the Monte Carlo simulation. R. Zeinali was a major contributor in processing films. H. Riazi-Esfahani was a major contributor in performing the experimental work. A. Beiki-Ardakani was a supporter and a major contributor in designing the manuscript. All authors read and approved the final manuscript.

Conflict of Interest

None

References

1. Singh AD, Turell ME, Topham AK. Uveal melanoma: trends in incidence, treatment, and survival. *Ophthalmology.* 2011;**118**(9):1881-5. doi: 10.1016/j.ophtha.2011.01.040. PubMed PMID: 21704381.

2. Virgili G, Gatta G, Ciccolallo L, Capocaccia R, Biggeri A, et al. Incidence of uveal melanoma in Europe. *Ophthalmology.* 2007;**114**(12):2309-15. doi: 10.1016/j.ophtha.2007.01.032. PubMed PMID: 17498805.

3. Kivelä T. The epidemiological challenge of the most frequent eye cancer: retinoblastoma, an issue of birth and death. *Br J Ophthalmol.* 2009;**93**(9):1129-31. doi: 10.1136/bjo.2008.150292. PubMed PMID: 19704035.

4. Stannard C, Sauerwein W, Maree G, Lecuona K. Radiotherapy for ocular tumours. *Eye.* 2013;**27**(2):119-27. doi: 10.1038/eye.2012.241. PubMed PMID: 23174750. PubMed PMCID: PMC3574242.

5. American Brachytherapy Society - Ophthalmic Oncology Task Force. The American Brachytherapy Society consensus guidelines for plaque brachytherapy of uveal melanoma and retinoblastoma. Brachytherapy. 2014;13(1):1-14. doi: 10.1016/j.brachy.2013.11.008. PubMed PMID: 24373763.

6. Zehetmayer M, Menapace R, Kulnig W. Combined local excision and brachytherapy with ruthenium-106 in the treatment of epibulbar malignancies. *Ophthalmologica.* 1993;**207**(3):133-9. doi: 10.1159/000310419. PubMed PMID: 8278179.

7. Cohen VM, Papastefanou VP, Liu S, Stoker I, Hunger-

ford JL. The use of strontium-90 Beta radiotherapy as adjuvant treatment for conjunctival melanoma. *J Oncol.* 2013;**2013**:349162. doi: 10.1155/2013/34916. PubMed PMID: 23431299. PubMed PMCID: PMC3572694.

8. Brewington BY, Shao YF, Davidorf FH, Cebulla CM. Brachytherapy for patients with uveal melanoma: historical perspectives and future treatment directions. *Clin Ophthalmol.* 2018;**12**:925-34. doi: 10.2147/OPTH.S129645. PubMed PMID: 29844657. PubMed PMCID: PMC5963830.
9. Echegaray JJ, Bechrakis NE, Singh N, Bellerive C, Singh AD. Iodine-125 brachytherapy for uveal melanoma: a systematic review of radiation dose. *Ocul Oncol Pathol.* 2017;**3**(3):193-198. doi: 10.1159/000455872. PubMed PMID: 29071269. PubMed PMCID: PMC5649338.
10. Wilkinson DA, Kolar M, Fleming PA, Singh AD. Dosimetric comparison of 106Ru and 125I plaques for treatment of shallow (≤ 5 mm) choroidal melanoma lesions. *Br J Radiol.* 2008;**81**(970):784-9. doi: 10.1259/bjr/76813976. PubMed PMID: 18628320.
11. Taccini G, Cavagnetto F, Coscia G, Garelli S, Pilot A. The determination of dose characteristics of ruthenium ophthalmic applicators using radiochromic film. *Med Phys.* 1997;**24**(12):2034-7. doi: 10.1118/1.598117. PubMed PMID: 9434987.
12. Gueli AM, Mannino G, Troja SO, Asero G, Burrafato G, De Vincolis R, et al. 3D dosimetry on Ru-106 plaque for ocular melanoma treatments. *Radiat Meas.* 2011;**46**(12):2014-9. doi: 10.1016/j.radmeas.2011.07.032.
13. Heilemann G, Nesvacil N, Blaickner M, Kostiukhina N, Georg D. Multidimensional dosimetry of 106Ru eye plaques using EBT3 films and its impact on treatment planning. *Med Phys.* 2015;**42**(10):5798-808. doi: 10.1118/1.4929564. PubMed PMID: 26429254.
14. Soares CG, Vynckier S, Järvinen H, Cross WG, Sipilä P, Flühs D, Schaeken B, Mourtada FA, Bass GA, Williams TT. Dosimetry of beta-ray ophthalmic applicators: Comparison of different measurement methods. *Med Phys.* 2001;**28**(7):1373-84. doi: 10.1118/1.1376441. PubMed PMID: 11488568.
15. Binder W, Chiari A, Aiginger H. Determination of the dose distribution of an ophthalmic 106Ru irradiator with TLDs and an eye phantom. *Radiation Protection Dosimetry.* 1990;**34**(1-4):275-8. doi: 10.1093/oxfordjournals.rpd.a080901.
16. Kaulich TW, Zurheide J, Haug T, Nüsslin F, Bamberg M. Clinical quality assurance for 106Ru ophthalmic applicators. *Radiother Oncol.* 2005;**76**(1):86-92. doi: 10.1016/j.radonc.2005.05.001. PubMed PMID: 15972240.
17. Davelaar J, Schaling DF, Hennen LA, Broerse JJ. Dosimetry of ruthenium-106 eye applicators. *Med Phys.* 1992;**19**(3):691-4. doi: 10.1118/1.596898. PubMed PMID: 1508109.
18. Lax I. Dosimetry of 106Ru eye applicators with a p-type silicon detector. *Phys Med Biol.* 1991;**36**(7):963-72. doi: 10.1088/0031-9155/36/7/005. PubMed PMID: 1886930.
19. Brualla L, Zaragoza FJ, Sauerwein W. Monte Carlo simulation of the treatment of eye tumors with 106Ru plaques: a study on maximum tumor height and eccentric placement. *Ocul Oncol Pathol.* 2014;**1**(1):2-12. doi: 10.1159/000362560. PubMed PMID: 27175356. PubMed PMCID: PMC4864522.
20. Hermida-López M. Calculation of dose distributions for 12 106Ru/106Rh ophthalmic applicator models with the PENELOPE Monte Carlo code. *Med Phys.* 2013;**40**(10):101705. doi: 10.1118/1.4820368.
21. Low DA, Harms WB, Mutic S, Purdy JA. A technique for the quantitative evaluation of dose distributions. *Med Phys.* 1998;**25**(5):656-61. doi: 10.1118/1.598248. PubMed PMID: 9608475.
22. Eckert & Ziegler. Fact Sheet: Ru-106 Eye Applicators. Berlin: Eckert & Ziegler BEBIG GmbH; 2021. Available from: https://www.bebig.com/fileadmin/bebig_neu/user_uploads/Products/Ophthalmic_Brachytherapy/Fact_sheet_Ru-106_Eye_Applicators__Rev.07__English_.pdf.
23. L'Annunziata MF. Handbook of radioactivity analysis. Academic Press; 2012. p. 1305-60.
24. Kok E, Geelen BP. IMRT pre-treatment verification using EBT3 film and FilmQA Pro software. Barcelona; 2012. Available from: http://www.gafchromic.com/documents/Kok_Poster_IMRT_EBT3_film_ESTRO_20120507.pdf.
25. Devic S, Tomic N, Lewis D. Reference radiochromic film dosimetry: review of technical aspects. *Phys Med.* 2016;**32**(4):541-56. doi: 10.1016/j.ejmp.2016.02.008. PubMed PMID: 27020097.
26. Schoenfeld AA, Poppinga D, Harder D, Doerner KJ, Poppe B. The artefacts of radiochromic film dosimetry with flatbed scanners and their causation by light scattering from radiation-induced polymers. *Phys Med Biol.* 2014;**59**(13):3575-97. doi: 10.1088/0031-9155/59/13/3575. PubMed PMID: 24909235.
27. Chavel P, Lowenthal S. Noise and coherence in optical image processing. I. The Callier effect and its influence on image contrast. *JOSA.* 1978;**68**(5):559-68. doi: 10.1364/JOSA.68.000559.
28. Agostinelli S, Allison J, Amako K, Apostolakis J, Araujo H, Arcel P, et al. Geant4–a simulation toolkit. *Nucl Instrum Meth A.* 2003;**506**(3):250-303. doi: 10.1016/S0168-9002(03)01368-8.
29. Sommer H, Ebenau M, Spaan B, Eichmann M. Monte Carlo simulation of ruthenium eye plaques with GEANT4: influence of multiple scattering algorithms, the spectrum and the geometry on depth dose profiles. *Phys Med Biol.* 2017;**62**(5):1848-64. doi: 10.1088/1361-6560/aa5696. PubMed PMID: 28050967.
30. Cember H, Johnson TE. Introduction to Health Physics: 4th ed. McGraw-Hill Companies; 2009.
31. Depuydt T, Van Esch A, Huyskens DP. A quantitative evaluation of IMRT dose distributions: refinement and clinical assessment of the gamma evaluation. *Radiother Oncol.* 2002;**62**(3):309-19. doi: 10.1016/s0167-8140(01)00497-2. PubMed PMID: 12175562.